Applied Catalysis A: General 467 (2013) 38–46

Contents lists available at ScienceDirect

Applied Catalysis A: General

journal homepage: www.elsevier.com/locate/apcata

Selective methoxylation of limonene over ion-exchanged and acid-activated clays

C. Catrinescu[a,b,*], C. Fernandes[a,c], P. Castilho[a], C. Breen[d], M.M.L. Ribeiro Carrott[e], I.P.P. Cansado[e]

[a] Centro de Química da Madeira (CQM), Centro de Ciências Exactas e da Engenharia da Universidade da Madeira, Campus Universitário da Penteada, 9000-390 Funchal, Portugal
[b] "Gheorghe Asachi" Technical University of Iasi, Faculty of Chemical Engineering and Environmental Protection, Department of Environmental Engineering and Management, 73 D. Mangeron Blvd, 700050 Iasi, Romania
[c] Laboratório Regional de Engenharia Civil, IP-RAM, Rua Agostinho Pereira de Oliveira, 9000-264 Funchal, Portugal
[d] Materials and Engineering Research Institute, Sheffield Hallam University, Howard Street, Sheffield, S1 1WB, UK
[e] Centro de Química de Évora and Departamento de Química, Universidade de Évora, Colégio Luís António Verney, 7000-671 Évora, Portugal

ARTICLE INFO

Article history:
Received 26 March 2013
Received in revised form 28 June 2013
Accepted 3 July 2013
Available online 13 July 2013

Keywords:
Ion-exchanged clays
Acid-activated clays
Catalysis
Limonene
Methoxylation
Terpinyl methyl ether

ABSTRACT

In this study, we report the use of clay-based catalysts in the methoxylation of limonene, for the selective synthesis of α-terpinyl methyl ether. Na-SAz-1, Ca-SWy-2 and Sap-Ca source clays and a montmorillonite (SD) from Porto Santo, Madeira Archipelago, Portugal were modified by (i) ion-exchange with Al, Fe, Ni and Na and (ii) acid activation, to produce catalysts with markedly different acidic and textural properties. The lack of activity of Ni^{2+}-SAz-1 (with Lewis acidity maximized), provided evidence that the process occurs preferentially on Brönsted acid sites. The catalysts based on the high layer-charge SAz-1 montmorillonite proved to be the most active. Ion-exchange with Al^{3+}, followed by thermal activation at 150 °C, afforded the highest number of Brønsted acid sites located in the clay gallery and this coincided with the maximum catalytic activity. The influence of various reaction conditions, to maximize limonene conversion and selectivity, was studied over Al-SAz-1. When the reaction was performed for 20 h at 40° C, the conversion reached 71% with 91% selectivity to the mono-ether. Mild acid activation (1 M HCl, 30 min, reflux) of the raw SAz-1 clay leads to a material with a good catalytic behaviour (slightly inferior to Al-SAz-1), while any increase in the severity of the acid-treatment (6 M HCl, 30 min, reflux), caused a marked decrease in catalytic activity.

1. Introduction

D-Limonene, a natural cyclic terpene, is the major constituent of citrus peel oils (90–95%) and the citrus industry produces 50,000 tonnes of limonene annually. Dipentene, a racemic mixture of D- and L-limonene, is recovered as a by-product from the distillation of turpentine oil and from the pulp and paper industry. In addition, smaller amounts of L-limonene can be distilled from oil of *Eucalyptus stageriana* [1]. As a renewable terpene, limonene can be used as a versatile building block for the synthesis of high-value added chemicals, mainly through catalytic processes. Indeed, the products of limonene alkoxylation, *1-methyl-4-(α-alkoxyisopropyl)-1-cyclohexenes*, are used as flavours and as fragrances for perfume and cosmetic products, as additives for pharmaceuticals and agricultural chemicals, and also in the food industry. Among these functionalized monoterpenes, the α-terpinyl methyl ether is of commercial interest due to its pleasant grapefruit-like aroma. Methoxylation of limonene over homogeneous (HCl, H_2SO_4, p-toluenesulfonic acid, aluminium trichloride and boron trifluoride etherate) or heterogeneous (acidic cation exchange resins, zeolites) catalysts have been reviewed by Hölderich and Heinz [2,3]. The use of strong homogeneous liquid acids is not recommended for industrial applications due to the associated corrosion and environmental challenges. Among the heterogeneous catalysts, zeolite beta exhibited the best performance, in terms of both activity (91.1%) and selectivity (93.2%), while USY and mordenite catalysts afforded a much lower activity. In contrast, ion-exchange resins and heteropoly-acids were quite active but offered only low selectivities, e.g. 61% and 5% respectively. A more recent study [4,5] confirmed the high activity and selectivity of beta-zeolite in the methoxylation of limonene.

Clay minerals, which cost considerably less than zeolites, are versatile and environmentally friendly catalysts that can be modified with relative ease to promote a wide variety of organic reactions [6]. First, the type of clay plays an important role in

* Corresponding author. Tel.: +40 232 237594; fax: +40 232 237594.
E-mail addresses: ccatrine@ch.tuiasi.ro, ccatrine@uma.pt (C. Catrinescu).

0926-860X/$ – see front matter © 2013 Elsevier B.V. All rights reserved.
http://dx.doi.org/10.1016/j.apcata.2013.07.012

Table 1
Chemical composition and the cation exchange capacities (CEC) for the host clays.

Clay	Chemical composition, % oxide								CEC(mEq 100 g^{-1})
	Na	Mg	Al	Si	K	Ca	Ti	Fe	
Na-SD	2.6	3.4	20.5	57.4	0.9	0.5	3.3	10.3	81
SAz-1	0.06	6.73	19.98	59.65	0.19	3.15	0.25	1.77	120
SWy-2	1.47	2.94	22.05	61.46	0.2	1.18	0.09	4.37	93
Sap-Ca	2.73	26.1	4.17	47.9	0.39	0.9	0.03	0.66	92

maximizing the catalytic activity for the precise reaction of interest. The nature, and extent, of the isomorphic substitution strongly influences the layer charge of the clay and both exert a major influence on the acidity and accessibility of the active sites. Furthermore, these natural attributes can be readily optimized using different methods such as *ion-exchange*, *acid treatment* and *pillaring* [7]. For example, Ni^{2+} and Al^{3+} exchanged montmorillonites are considered model Lewis and Brønsted acids, respectively. The nature of the active sites has been unequivocally determined using FT-IR spectra of adsorbed pyridine [8] and verified by catalytic data. *Acid treatment* of clays results in two major outcomes: the replacement of the exchangeable cations by protons and the dissolution of metals ions from the clay structure, by depopulating the octahedral sheet. The severity of the acid treatment needs to be optimized for a particular clay and is determined principally by the nature of the ions occupying the octahedral sheet. Clays rich in octahedral Al are more resistant to acid dissolution than those rich in Fe, whereas large octahedral Mg populations make clays extremely susceptible to acid leaching. The acid activated materials produced are not stable in the H-form [9], due to gradual exsolution of metal ions from the octahedral sheet which displace the protons on the cation exchange sites (clay autotransformation). Acid activation alters the number, strength and, perhaps, also the type of acid sites on the clay. Removal of ions from the octahedral sheet leads to an initial increase in the surface area, followed by a simultaneous decrease in both cation exchange capacity, CEC, and surface area under more severe treatment conditions. The resulting open porous structure can make a higher number of acid sites available to reagents that are not sufficiently polar to enter the gallery and swell the untransformed part of the clay beyond the frontier of acid attack.

The primary goal of this work was to evaluate the activity and selectivity of clay-based catalysts, as an economically attractive alternative to beta-zeolite, for the alkoxylation of limonene. A particular focus of the work is to explore how the nature of the source clay together with the clay activation method influences the activity toward the production of the limonene ether. A second aim is to understand the role of key factors considered to control the activity and the selectivity toward the desired product: the role of the controlling reaction environment (2-D as in clay galleries or 3-D as in mesopores), the acidity (nature, density and strength) of the catalysts' surface. These features have been proved to be of equal importance for liquid phase reactions involving reactants of different polarity [10].

2. Experimental

SAz-1 (Cheto, Arizona, USA) and SWy-2 (Wyoming, USA) montmorillonites and Sap-Ca (Ballarat, California, USA) saponite were received from The Clay Mineral Society Source Clay repository (Purdue University). K10 acid activated clay, derived from the Bavarian montmorillonite Tonsil 13, was provided by Sud Chemie AG. The raw bentonite (SD) was collected from the Serra de Dentro deposit (Porto Santo – Madeira Archipelago, Portugal) and purified as previously described [16] to give the purified Na-SD form, which was used to prepare all the cation-exchanged forms of SD. The chemical composition and the cation exchange capacities (CEC) for the host clays are listed in Table 1.

2.1. Catalyst preparation

2.1.1. Ion-exchanged clays

Cation exchange of the clay was carried out by stirring a 1% suspension of a previously prepared Na-saturated form of the clay overnight in 0.3 M solution of the desired cation (Al^{3+}, Fe^{3+}, Ni^{2+}). The suspensions were then centrifuged and the resulting pellets washed with de-ionized water, dried, ground and stored in closed vials. The ion-exchanged clays are denoted by their interlayer cation followed by code of the host clay, e.g., Al-SD is the Al^{3+} ion-exchanged form of purified Na-SD clay; Fe-SapCa is Fe-exchanged saponite and Na-SAz-1 is the Na-exchanged form of SAz-1.

2.1.2. Acid activated clays

Acid activated (AA) samples were prepared by stirring 10 g of clay (Na-SAz-1) with 300 ml aliquots of aqueous HCl (of the required concentrations) at 95 °C, for 30 min. The samples were then diluted with a large quantity of cold water to effectively terminate the leaching process, centrifuged and washed successively until a stable pH was achieved. The samples were air-dried for 24 h. Samples are labeled as: acid concentration–temperature of activation–contact time in minutes. For example, SAz-6M-95-30 is the material obtained when a 10 g sample of Na-SAz-1 was treated with 6 M HCl at 95 °C, for 30 min. The same procedures were applied to SD.

2.2. Catalyst characterization

The XRD patterns were recorded using a Shimadzu LabX XRD-6000 diffractometer with Cu $_{K\alpha}$ radiation (λ = 1.54184 Å). The nitrogen adsorption–desorption isotherms at −196 °C were determined, using helium (for dead space calibration) and nitrogen of 99.999% purity, on a Autosorb-iQ and some also on a Quadrasorb-*SI*, both from Quantachrome Instruments and equipped with turbomolecular pumps to attain high vacuum, using helium (for dead space calibration) and nitrogen of 99.999% purity. Prior to the adsorption measurements, all the samples were outgassed for 5 h at 200 °C, achieved using a heating rate of 1 °C min^{-1}.

TG data were recorded on a Mettler TG50 thermobalance equipped with a TC10A processor. Samples (∼10 mg) were transferred directly out of cyclohexylamine, CHA, vapour into the thermobalance and the desorption traces were recorded at a heating rate of 20 °C under a nitrogen flow of 25 cm^3 min^{-1}. Samples were conditioned for 15 min under flowing nitrogen to reduce the amount of physisorbed CHA. Variable temperature diffuse reflectance infrared Fourier transform spectra (VT-DRIFTS), were recorded at room temperature, then at 25 °C increments until 200 °C followed by 50 °C increments until 500 °C. Samples were held at a specific temperature for 15 min in a flow of dry nitrogen in a variable-temperature cell (Graseby-Specac; maximum operating temperature 500 °C). The spectrometer used was a Mattson Polaris operating at 4 cm^{-1} resolution and 256 scans.

2.3. Catalytic tests

Limonene and n-decane (internal standard), used as received from Aldrich, were dried over anhydrous magnesium sulphate. Alcohols were dried over 3A molecular sieve. Before reaction, a known amount of catalyst was thermally activated at 150 C, in air, for 2 h in a vial. Before being removed from the oven, the vials were stoppered and then placed in a dessicator to cool and prevent rehydration. After being cooled at room temperature (15 min) dry methanol was injected first, followed by limonene and n-decane (internal standard). The glass vials were transferred to an oil bath, preheated at the reaction temperature and this marked the start of the reaction. After the reaction, the vials were cooled, opened and the catalyst was removed by syringe filtration. The filter had no influence on the reaction products and no further reaction took place during storage. The reaction products were identified by GC–MS (Varian Saturn 3) and quantified by GC with FID, using the n-decane internal standard.

3. Results and discussion

3.1. Catalyst characterization

3.1.1. X-Ray diffraction (XRD)

The XRD trace of the unpurified SD confirmed that montmorillonite was the major component and magnesian calcite (C) the major impurity together with smaller amounts of anorthite (A), feldspar (F) and quartz (Q) (Fig. 1). The basal reflection of the raw SD sample occurred at 5.89° 2θ (15.0 Å) indicating the presence of two layers of molecular water in the interlamellar space. The characteristic non-basal reflections (hk bands) were found at 19.8° 2θ (4.47 Å), 35.0° 2θ (2.56 Å), and 61.86° 2θ (1.5 Å). The XRD trace for the purified Na-SD pattern, collected at 10% RH, demonstrated that most of the impurities had been removed, the characteristic hk bands remain unchanged while the basal reflection decreased to 7.1° 2θ (12.45 Å) reflecting the loss of interlayer water at this low humidity.

Al-SAz-1 displays a well defined d_{001} reflection indicating a well-ordered arrangement of the clay platelets. Following acid activation, the intensity of the basal reflection diminished with increasing severity of acid treatment, with SAz-6M-95-30 exhibiting a weak, broad reflection. The non-basal reflections were much less affected by the acid treatment. Acid activated samples retained some of their crystalline character even when treated with 6 M acid.

Table 2
Results of the analysis by the BET method of the nitrogen adsorption isotherms determined at −196 °C on selected clay materials.

Sample	A_s (BET)/m^2 g^{-1}	C (BET)
SD raw	110	252
Na-SD	118	250
Al-SD	140	329
Al-SapCa	13	60
Al-SWy-2	33	142
Al-SAz-1	96	490
SAz-1M-95-30	169	288
SAz-3M-95-30	353	163
SAz-6M-95-30	442	148

3.1.2. Nitrogen adsorption

The textural properties of SD, Al^{3+}-exchanged clays and acid-activated SAz-1 samples were investigated using nitrogen adsorption at −196 °C and the values obtained by applying the BET method [30] to the corresponding isotherms are presented in Table 2. Some representative adsorption–desorption isotherms are presented in Fig. 2.

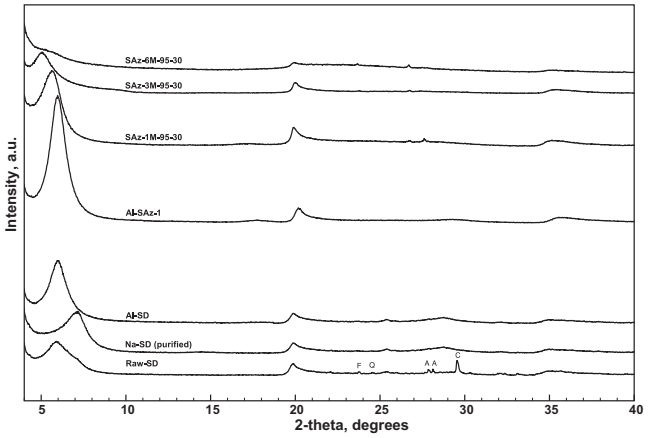

Fig. 1. X-Ray diffraction patterns of selected catalysts based on SD and SAz-1 clays.

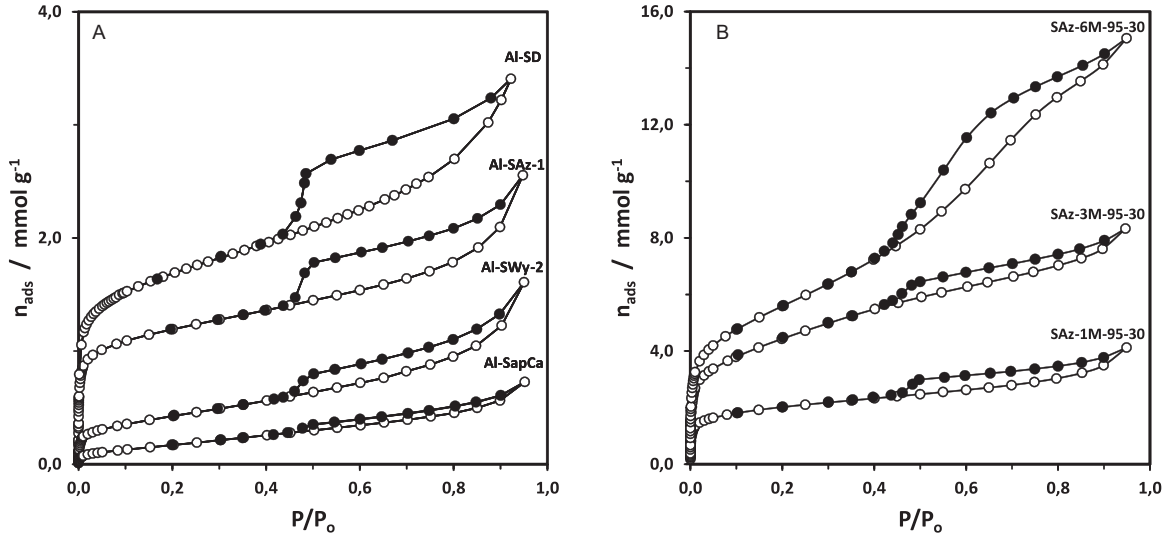

Fig. 2. Nitrogen adsorption–desorption isotherms determined at −196 °C on: (a) Al^{3+} exchanged clays; (b) acid activated SAz-1. (Empty symbols: adsorption, filled symbols: desorption).

At high relative pressures the isotherms of aluminium exchanged clays approach type IIb [31] and exhibit hysteresis loops typical for materials having slit-shaped pores between plate-like particles [31,32]. Some hysteresis loops are more pronounced than others which may be due to distinct microstructures [11]. The observed increase in specific surface area for Na-SD may be linked to the removal of impurities present in the raw bentonite. Significant differences are observed among the specific surface areas of the Al exchanged clays, with those of Al-SD and Al-SAz-1 being larger. This is likely to be due to the presence of micropores, in particular narrow micropores, as evidenced by the steep low pressure region of the isotherms and by the higher values of C (BET) in Table 2.

The SAz-1 samples activated using 1 M and 3 M acid exhibited the same type of isotherm and hysteresis loop as those in the SD samples and the as-received SAz-1 material. In contrast, the isotherm for the more harshly treated sample (SAz-6M-95-30) shows a rather irregular hysteresis loop at $P/P_0 > 0.4$. This transformation of the hysteresis loop, partially associated with ink-bottle shaped pores, is generally attributed to the onset of a 3-D silica structure. An increase in the acid concentration lead to a considerable increase in the specific surface area and to the decrease of the C (BET) values, but the nitrogen adsorption isotherms exhibit, at low relative pressures, some type I character. In order to explain the textural changes that take place during the acid treatment, it is important to remember that, in smectites, most of the specific surface area is attributed to micropores present in the intraparticle space in "quasi crystalline overlap regions" and from the interlayer space at particle edge surfaces of swelling clay minerals which is partly accessible to N_2 [11–13]. The total specific surface area might also be affected, to a smaller extent, by the arrangement of the particles with respect to each other (microstructure) [11]. Acid activation is most pronounced around the periphery, consequently the edges of clay platelets open up and separate while the comparatively pristine regions at the centre of the platelets remain closely associated. The N_2-accessible interlayer space at the particle edge increases as the acid concentration increases, leading to a higher, measurable specific surface area (Table 2). This area is also accessible to non-polar molecules that are not able to penetrate into the interlayer region. However, in this region (the splayed layers at the edge) the number of the acid sites is strongly diminished, because the "opening" of the structure is a direct consequence of the dissolution of the octahedral cations (Mg, Fe) which are the origin of the negative charge on the clay layers. These textural changes are known to strongly influence the catalytic properties of clays (see below).

3.1.3. Pyridine VT-DRIFTS

VT-DRIFTS of pyridine treated samples still remains the standard way to unequivocally distinguish between Brønsted and Lewis acid sites on the surface of solid acid catalysts [8]. It has been shown [14] that peaks at 1635 and 1540 cm^{-1} can be assigned to the pyridinium ion (Brønsted acidity, BPYR), whereas peaks at 1613 and 1450 cm^{-1} are diagnostic for pyridine co-ordinately bound to Lewis acid sites (LPYR) while peaks at 1596 and 1440 cm^{-1} may report the presence of H-bonded pyridine (HPYR). All these species contribute intensity to the 1490 cm^{-1} band although the largest contribution at higher temperatures (>120 °C) is from BPYR. In accordance with our previous studies [16] Al-exchanged clays exhibited bands associated with BPYR (and some minor LPYR) while for Ni-SAz-1 bands associated with LPYR (Fig. 3) dominated the spectrum.

The spectra obtained from the Al-SAz-1 sample revealed sharper and better defined peaks than those from the corresponding sample derived from SD which probably indicates a more uniform distribution of the acid site strength on SAz-1 than on SD.

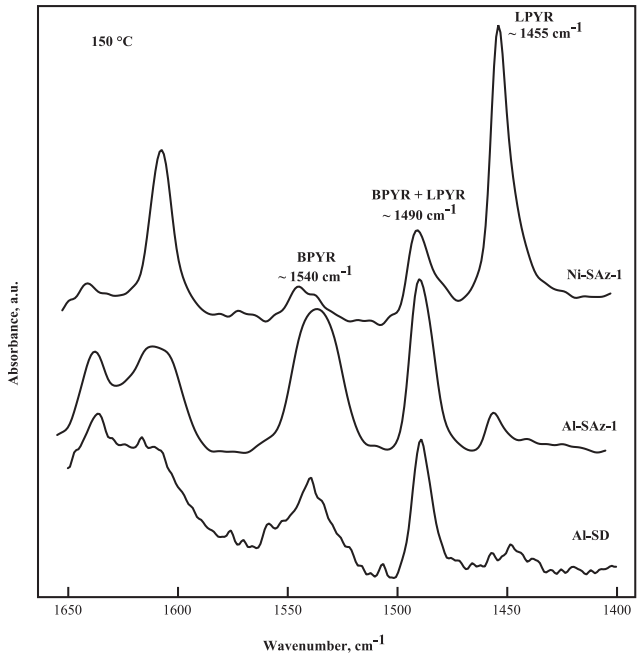

Fig. 3. DRIFTS spectra of pyridine adsorbed on Al-SD, Al- and Ni-SAz-1 after evacuation at 150 °C.

3.1.4. Thermogravimetric (TG) studies

It has been suggested that the thermal desorption of cyclohexylamine can be used to quantify the number of acid sites on a clay catalyst [15]. The technique requires the determination of the weight loss between 280 and 440 °C and its conversion to the number of mmol of CHA desorbed. The relative ease of obtaining this quantity has popularized its use even though the value obtained does not distinguish between cyclohexylamine bound to Brønsted or Lewis acid sites. Moreover, the method often reports high acidity values which are not substantiated by the yields obtained in the associated tests of catalytic activity. For example, the presence of Ca^{2+}-ions, which retain CHA to temperatures at which thermal C—N bond cleavage occurs, can lead to a spurious acidity value [25]. The quantities of CHA desorbed in the appropriate temperature interval are presented in Table 3.

As expected, Na-SAz-1 exhibited a very weak peak at 325 °C (0.15 mmol CHA g^{-1}), but Na-SD presented a more intense peak than expected for a Na^+-exchanged clay (0.56 mmol CHA g^{-1}). With the exception of the Na form, the SD clays generally desorb lower quantities of CHA than the equivalent SAz-1 samples, which correlated well with the difference in CEC between SAz-1 (120 meq 100 g^{-1}) and SD (80 meq 100 g^{-1}). Concerning the acid activated clays, the quantities of CHA desorbed in the appropriate temperature interval (Table 3) show, as anticipated from earlier work [28],

Table 3
Cyclohexylamine (CHA) thermodesorption.

Nr. Crt	Sample	CHA (mmol g^{-1})	T (max)
1	Na-SAz-1	0.15	325
2	Al-SAz-1	1.64	270, 316, 354
3	Ni-SAz-1	1.21	352
4	Na-SD	0.56	325
5	Al-SD	1.2	325
6	Al-SWy-2	1.46	325
7	Al-SapCa	1.32	320
8	SAz-1M-95-30	1.036	326, 362
9	SAz-3M-95-30	0.94	332
10	SAz-6M-95-30	0.374	352

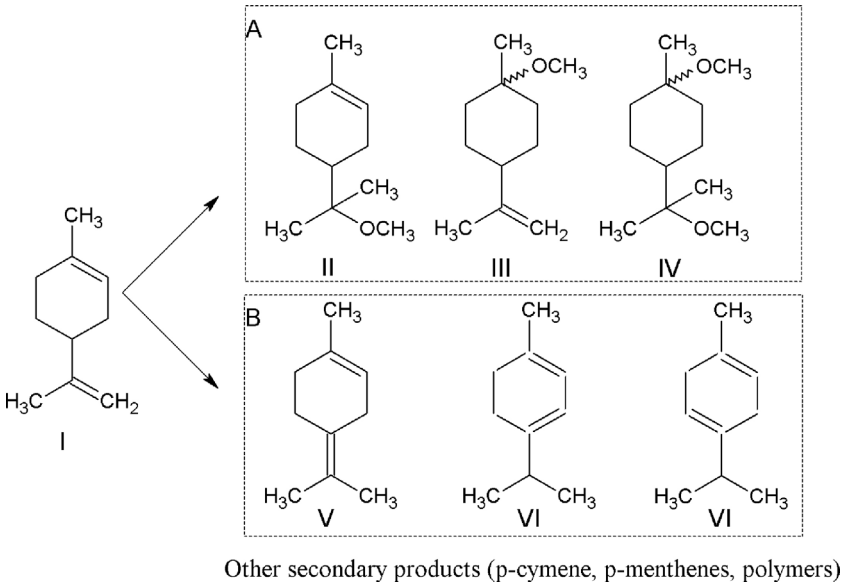

Scheme 1. Main reaction products in the methoxylation of limonene.

that the estimated acidity values decreased as the severity of the acid treatment increased.

3.2. Reaction products and intermediates

In the presence of acidic sites available at the clay surface, limonene reacted to form a mixture of products, as shown in Scheme 1. Two main reaction pathways could be distinguished. The major one (A) involves the addition of the alcohol leading to the main product, α-terpinyl methyl ether (II) and to smaller amounts of β-terpinyl methyl ether (III) and *cis* or *trans* 1,8,-di-methoxy-p-menthanes. (IV) The second reaction pathway (B) proceeds via isomerization/disproportionation/polymerization and leads to isomeric terpenes (terpinolene (V), α-terpinene (VI) and γ-terpinene (VII), isoterpinolene), high molecular-weight compounds, p-cymene and p-menthenes [11].

The main reaction intermediates (Supplementary information) were identified from their mass spectra. Thus, the mass spectrum of the mono-ether [II] displayed a molecular ion M^+ of low intensity at *m*/*z* 168, followed by specific fragments at *m*/*z* 153 (M^+-CH_3), 136 (M^+-CH_4O) and 121 (M^+-CH_4O-CH_3) and the base peak at *m*/*z* 73 corresponding to $C(CH_3)_2OCH_3$ or (M^+-C_7H_{11}). The two diether isomers (III and IV) produce similar mass fragments to the mono-ether, but with a molecular ion at *m*/*z* 200 together with an ion at *m*/*z* 185 (M^+-CH_3).

Fig. 4 uses the catalytic test results, obtained over Al-SAz-1 following pre-treatment at 150 °C, to illustrate how the total limonene conversion and product distribution varied with time. The conversion, selectivity and composition of the reaction mixture, after 16 h of reaction, are presented in Table 4. The initial increase in limonene conversion, after 1 h of reaction, is accompanied by the selective production of α-terpinyl methyl ether (II), the only primary product of reaction. At this point in the reaction, no secondary products were detected. As limonene conversion increased and the mono-ether accumulated in the reaction system, additional alkoxylation products (mono and di-ethers) were formed, together with the isomeric terpenes identified in Scheme 1B.

In order to explain these observations it is reasonable to assume that methanol, due to its polarity, will be preferentially adsorbed by the clay. Previous studies [17] showed that methanol is able

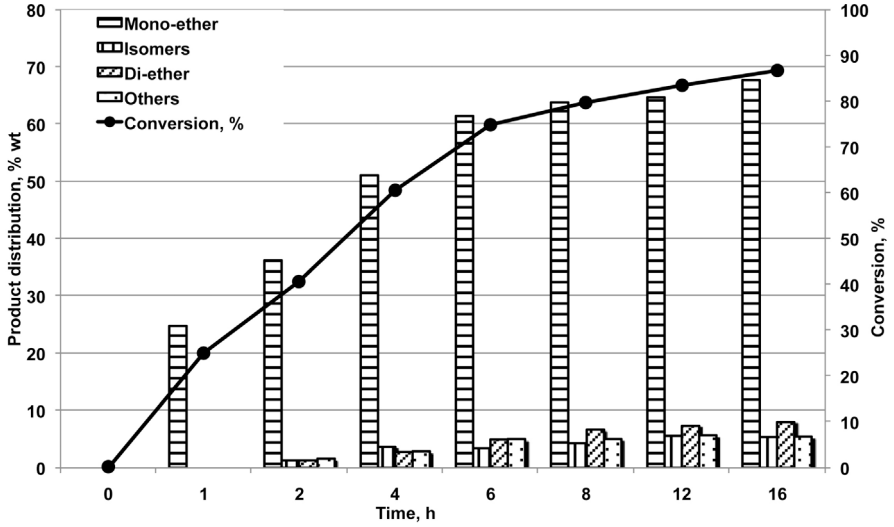

Fig. 4. Limonene conversion and product distribution at different reaction times. Reaction conditions: 200 mg Al-SAz-1, 60 °C, 1 ml MeOH, 0.5 ml Limonene.

Table 4
Product distribution, limonene conversion and selectivity to α-terpinyl methyl ether over Al-SAz-1. Reaction conditions: 200 mg Al-SAz-1, 16 h, 60 °C, 1 ml MeOH, 0.5 ml Limonene.

Product	Composition (%wt.)
Limonene	13.25
α-Terpinene	2.9
γ-Terpinene	1.8
Terpinolene	0.8
Mono-ether	67.8
Di-ether	8.07
Others	5.37
Limonene conversion, %	86.75
Selectivity, %	78.16

to penetrate into the interlamellar space of the clay and solvate the exchange cations (by dipole-cation interactions of the oxygen lone pair of electrons with the empty electronic orbitals of the charge-balancing cations). The protons generated by the polarization of water or methanol by the metal cations will protonate limonene, leading to the terpinyl ion. Another possibility is the generation of methoxonium ions from methanol, which will act as the protonating agent of limonene, leading to the same terpinyl ion. In the presence of excess methanol, the methoxonium cation will react quickly, forming mainly α-terpinyl methyl ether. The same carbocation could be involved in a series of isomerization, polymerization and hydrogen shift reactions, with the production of isomeric terpenes (terpinolene, α-terpinene, γ-terpinene), p-cymene, p-menthenes and other oligomers/polymers. However, in the early stages of the process the products from these reactions are negligible. As the mono-ether content increases, secondary alkoxylation products, e.g. di-ethers are formed, together with some isomeric terpenes. This could possibly indicate that the limonene isomers are actually secondary reaction products, arising from decomposition of the ether into alcohol and limonene isomers.

Moreover, as the methanol is consumed and more ether is formed, the reaction medium in the gallery will become less polar and more favorable to limonene adsorption and conversion, through secondary reactions (isomerization).

Unreacted terpenes were present in the final reaction mixture, even after an extended reaction time (16 h). This, together with the failure to increase the yield of the ether at longer reaction times, confirms the equilibrium nature of the process as already identified in the homogeneous process [18].

Although the etherification reaction involves an equilibrium, this is not the only factor limiting the yield of mono-ether. The initial supposition was that secondary reactions, involving the generation of limonene isomers, are of equal significance because they produce isomeric terpenes, which are less reactive in the alkoxylation process. In order to confirm this assertion, α-terpinene and terpinolene (the main isomers identified in the product mixture) were used as the starting terpenes rather than limonene. Both isomers failed to react with methanol to produce the ether and did not participate in other carbocation initiated transformations. The lack of isomerization could be considered a direct manifestation of the inhibiting effect of methanol. Due to its high polarity and weak acidity (in the protonated form) the reactions involving the protonation of the selected isomeric dienes were suppressed. The inhibiting effect of some polar alcohols on the conversion of C5- and C8-alkenes has been previously reported [19]. It is also worth noting that α-terpinene was found to be more reactive in the acid-catalyzed isomerization than limonene. Terpinolene and limonene have similar reactivity, although the former was slightly less reactive in the first stage of the isomerization process [20]. This may suggest that the process does not proceed through proton transfer to the terpene molecule, with the formation of the free carbocation. It is also an additional proof that limonene isomers are secondary reaction products. A one-step concerted mechanism, where the transfer of the methoxy group occurs simultaneously with the transfer of the proton is an attractive interpretation. This process seems to occur only for limonene but not for terpinolene. Both molecules have identical C1—C2 endocyclic bonds but different exocyclic bonds (C8—C9 in limonene and C4=C8 in terpinolene).

The most important feature of this catalytic system is the high selectivity toward the main product, α-terpinyl methyl ether, especially at low limonene conversions. This behaviour contrasts with that of some strong acids (polyoxometalates, ion-exchange resins and some zeolites) when isomerization/disproportionation/polymerization processes occur during the early stages of reaction [2,21]. This system is of considerable practical importance because it offers good selectivity toward the mono-ether, even at high limonene conversion.

3.3. Reaction parameters

The influence of the temperature, amount of clay and reaction time was followed over Al-SAz-1 catalyst. The influence of the temperature on limonene conversion and selectivity toward the mono-ether (Table 5; rows 1–5) shows that the optimum is around 40 °C, for long reaction times. At this temperature (row 3), a good selectivity, (ca. 91%) at 71% conversion of limonene was obtained. Satisfactory results were also obtained at 60 °C, albeit at shorter reaction time (6 h), when the selectivity reached 82% at 75% limonene conversion (Fig. 4). Above 60 °C the limonene conversion rate increases but the selectivity drops dramatically. This is due to the consecutive reaction, resulting in the formation of the di-ether and to the decomposition of the mono-ether into limonene isomers and alcohol. At 80 °C, two additional products were identified in the final reaction mixture: p-cymene and high molecular-weight compounds. The first could arise from disproportionation on acid sites or by oxidation on redox sites (e.g., structural iron in the clay) while the non-volatile fraction could be formed by polymerization of dienes on the acid sites.

The effect of the alcohol/limonene (ROH/L) ratio is presented in Table 5, rows 3, 6 and 7. By reducing the ROH/L mass ratio, from 2 ("normal" value) to 1 the limonene conversion decreased significantly. At this concentration the formation of two liquid phases was observed and mass transfer could have limited the overall conversion.

Doubling the amount of alcohol did not provide any real improvement giving only a small increase in limonene conversion with an attendant decrease in selectivity toward the mono-ether.

The amount of the catalyst was varied between 100 and 300 mg and the conversion increased as more catalyst was used, at constant reaction time.

3.4. Nature of the clay

Fig. 5 presents the limonene conversion and the product distribution for Al-exchanged clays prepared from different starting materials (Table 1), after thermal activation at 150 °C. Over these clay catalysts, limonene reacts promptly with dry methanol to yield the corresponding α-terpinyl methyl ether, as the main reaction product with selectivity in excess of 80%.

Clearly, the type of the clay has a profound effect upon the catalytic activity. Catalytic activities over clays, whether they arise from Brønsted or Lewis acidity, generally correlate with the cation-exchange capacity (CEC) of the base clay, provided the reactant can enter the gallery. Thus, SAz-1, a well-known montmorillonite of relatively high CEC (120 meq 100 g^{-1} clay), would provide more acid sites than similarly exchanged SWy-2, Sap-Ca and SD samples (Table 1). SWy-2 and Sap-Ca have similar CEC (87 and 92 meq

Table 5
The influence of the reaction temperature, amount of catalyst and reaction time on limonene conversion and selectivity to α-terpinyl methyl ether.

Nr. Crt.	Temperature (C)	Catalyst (mg)	Time (h)	Conversion	Selectivity
1	25	200	20	18.20	100
2	40	200	20	51.04	100
3	40	300	20	70.86	90.84
4	60	200	20	86.75	78.16
5	80	100	20	89.20	40.81[a]
6[b]	40	300	20	37.40	100
7[c]	40	300	20	71.80	83.96

Al-SAz-1 was used as catalyst.
[a]Composition of the final reaction mixture: 8.9% α-terpinene, 10.8% Limonene, 3.1 γ-terpinene, 1.42% p-cymene, 6.8% terpinolene, 1.7% isoterpinolene, 36.4% mono-ether, 11.1% di-ether, 19.7% others (mainly high molecular weight compounds). [b]ROH/L= 1; [c]ROH/L = 4

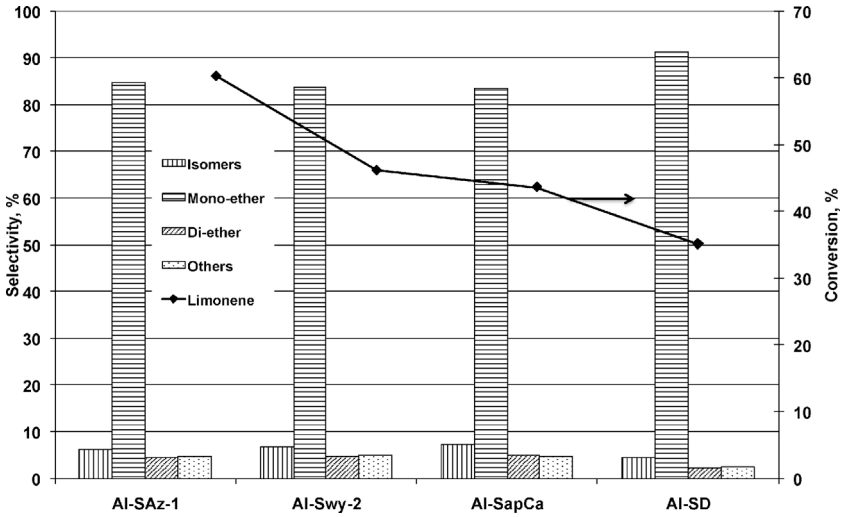

Fig. 5. Limonene conversion and product distribution over Al^{3+}-exchanged catalysts prepared from different starting clays. Reaction conditions: 200 mg catalyst, 60 °C, 4 h, 1 ml MeOH, 0.5 ml Limonene.

100 g^{-1} clay) and give similar conversions (46.2 and 43.6%) and product distributions. SD clay, having the lowest CEC (81 meq 100 g^{-1} clay), was the least active catalyst, affording a lower conversion than SAz-1. The catalytic activities toward this reaction seem to reflect the relative abundance of acid sites on the catalyst surface. Thus, for Al^{3+}-exchanged clays the order of activities is the same as the order of acid site concentrations, as determined by CHA desorption experiments (Table 3), which is also related to the CEC of the starting clay.

It is evident that the values of the selectivity toward α-terpinyl methyl ether are similar (Fig. 8), irrespective of the nature of the host clay, suggesting that the same mechanism was operating. This is consistent with the proposed model, with protons being produced from water molecules strongly polarized by exchangeable cations present in the interlayer space of the clay.

3.5. Exchange cation – the nature of the active sites

Fig. 6 illustrates the activity and selectivity obtained over Al^{3+}-, Fe^{3+}-, Ni^{2+}-exchanged SAz-1 catalysts, in comparison with the benchmark Na^{+}-SAz-1, after 120 min of reaction at 80 °C.

The acidity of clays ion-exchanged with these particular cations is well documented. Thus, Breen [8] and Brown and Rhodes [22] showed that Al^{3+} and Fe^{3+}-montmorillonites, after thermal activation at $T < 150$ °C, offered predominantly Brønsted acid sites, while Ni^{2+} -exchanged forms contained Lewis acid sites. Moreover, Brown and Rhodes [22] proved that Al-exchanged K10 clay exhibits stronger Brønsted sites than its Fe-exchanged counterpart.

Our previous VT-DRIFTS studies on pyridine-treated ion-exchanged samples confirmed the overall dominance of bands associated with pyridinium ion (Brønsted acid sites; 1540 cm^{-1}) in Al-exchanged clays, in contrast to Ni-exchanged clays, in which well-defined bands, attributed to pyridine coordinately bound to Lewis sites, were observed [11]. Conversely, Na-SAz-1 showed little to no evidence of the presence of Brønsted or Lewis acid sites.

The marginal catalytic activity over Na-SAz-1 suggests that the active sites are associated with the exchangeable cations, located mainly in the clay gallery. The Fe^{3+} and Al^{3+}-exchanged samples displayed similar activities and selectivities, while Ni-SAz-1 displayed very little to no activity. This clearly proves that the reaction is taking place on Brønsted sites, associated with the exchange

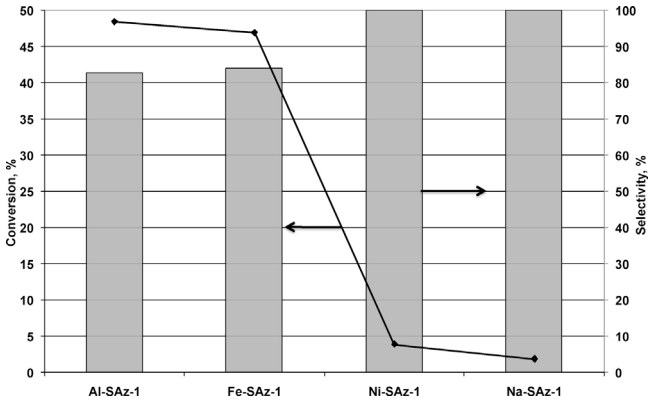

Fig. 6. The influence of the nature of the exchange cation on SAz-1 on limonene conversion and selectivity toward α-terpinyl methyl ether. Reaction conditions: 100 mg catalyst, 80 °C, 2 h, 1 ml MeOH, 0.5 ml Limonene.

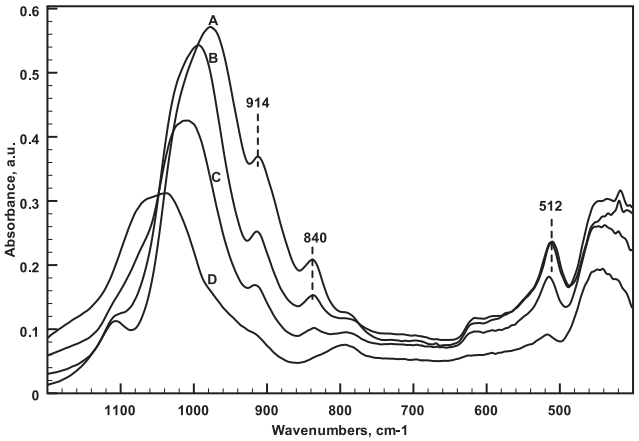

Fig. 7. FTIR spectra of (A) SAz-1, (B) SAz-1M-95-30, (C) SAz-3M-95-30 and (D) SAz-6M-95-30.

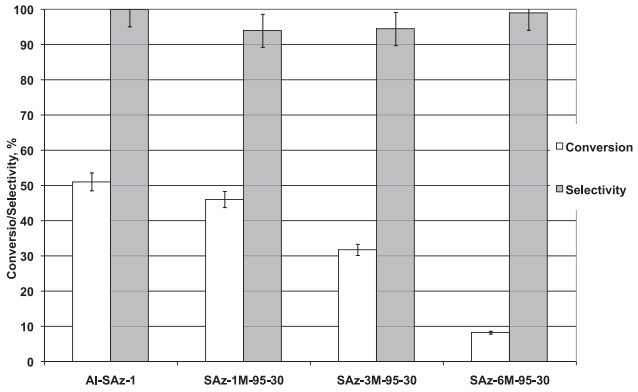

Fig. 8. The influence of the acid activation conditions on limonene conversion and selectivity toward α-terpinyl methyl ether. Reaction condition: 200 mg catalyst, 40 °C, 20 h, 1 ml MeOH, 0.5 ml Limonene.

cations. Accepting the previous findings, that Fe^{3+} and Al^{3+} generate Brønsted acid sites of different strength [23], it would appear that the relative strengths of acid sites on the catalysts surface have little influence on the catalytic activity. The attenuation of the acid strength, due to the solvation of the active cations with methanol, could explain the identical activities obtained over these catalysts. In marked contrast, Ni-SAz-1 has very little to no activity at all. The poor activity of Ni-exchanged clays in Brønsted-catalysed reaction has been observed before [18]. The dominance of Lewis acid centres on these catalysts, with a marginal number of Brønsted sites (Fig. 3), could justify the observed catalytic activity.

3.6. Acid activated clays

The acid treatment conditions used to maximize the catalytic activity of raw clays depend on the reaction system studied. Thus, in the presence of a polar (swelling) reagent, mild activation conditions are suitable, resulting in a high number of acid sites located in the interlayer region of the clay. In contrast, for non-polar molecules, severely acid treated clays are more effective since they offer a high number of external sites, accessible to the non-polar molecules [24].

Preliminary studies used an acid-treated montmorillonite (K10), a well-defined and reliable material, was introduced as a reference material. Unfortunately, K10 proved to be a poor catalyst for the alkoxylation of limonene. This was attributed to the reduced number of acid sites in the residual interlayer region of the clay, rather than the higher surface area and more accessible sites on the surface resulting from acid treatment. Thus, in an effort to further corroborate the critical contribution from the acid sites in the 2-D clay gallery, samples of Na-SAz-1 were acid leached under increasingly severe conditions.

The FTIR spectra presented in Fig. 7 illustrate the structural transformations that the SAz-1 structure undergoes, as the concentration of the HCl solution used in the acid-activation process is increased.

The spectra of the acid leached SAz-1 materials (Fig. 7) revealed different extents of structural modification, in direct correlation with the concentration of the acidic solution. As expected, the IR spectra of SAz-1 derived samples closely resembled those for corresponding samples prepared by Komadel et al. [25] and Breen et al. [24,26,27]. No significant changes were observed in the IR spectrum of SAz-1M-95-30 (Fig. 7B), apart from a slight decrease in the intensity of both OH bending vibrations (918 and 840 cm^{-1}), which reflects the reduction in content of the octahedral cations. Acid treatment with 3 M (Fig. 7C) and 6 M HCl (Fig. 7D) solutions produced increasingly more dramatic changes in the clay structure. The OH bending vibrations continue to decrease in intensity for the former, and are undetectable for the latter. The 516 cm^{-1} band, which is the most sensitive indicator of the presence/absence of octahedral aluminium in acid-treated montmorillonites, decreased in intensity for SAz-3M-95-30 and almost disappeared for SAz-6M-95-30. A mild acid treatment, as in the case of SAz-1M-95-30, is known to produce a catalyst with negligibly affected layers. The contact with 3 M HCl solution caused substantial depletion of the SAz-1 octahedral sheet maintaining, however, an important fraction of the clay structure present in the original material. The most severe acid treatment almost destroyed the clay structure.

Fig. 8 illustrates the effect of the degree of acid activation of SAz-1 clay on limonene conversion and selectivity. The catalytic activity for acid activated samples decreased with increased severity of the acid treatment. SAz-1M-95-30 was almost as active as the Al-exchanged form. This is in agreement with the acidity measurement using CHA thermodesorption (Table 3), which showed that the number of acid sites (1.036 mmol g^{-1} clay) was lower than that of the Al-exchanged clay (1.42 mmol g^{-1} clay). By increasing the severity of the acid treatment, the total number of acid sites located in the 2-D clay gallery is expected to decrease, as a consequence of the depletion of the octahedral cations, causing a negative impact on the catalytic process. It is also important to note the high values for the selectivity toward the mono-ether. This could be an indication that the acid sites generated on the external surface of the clay, by acid activation, although accessible to non-polar limonene molecules, do not contribute much to the isomerization/disproportionation/polymerization reactions. In this context, it is significant to mention that these external sites were particularly active in the conversion of limonene over acid activated clays, in a non-polar reaction system [28]. It seems that, similarly to the ion-exchanged clays, the solvation of the exchangeable cations by methanol could exert a leveling effect on the strength of the acid sites. From these data it seems that (i) the key factor which controls the catalytic activity is the total number of the Brønsted acid sites, located in the gallery and (ii) the simultaneous increase in surface area and the generation of a mesoporous structure seem to have no positive influence on the reaction, confirming the reaction takes place in the interlayer space of the clay. Thus, the existence of a 2-D reaction space, offered by the clay gallery, seems to be critical in getting the reagents in close proximity and the correct orientation to promote the required transition state.

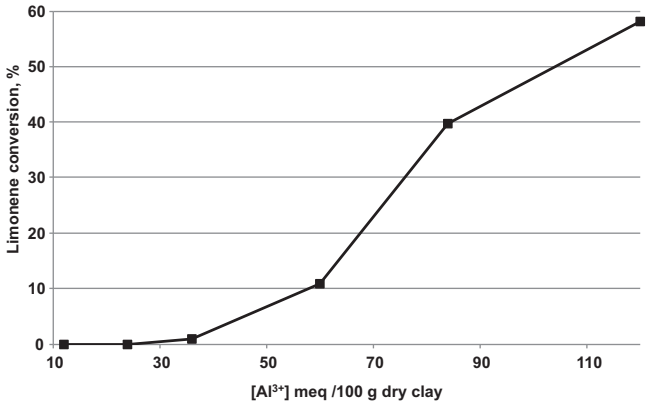

Fig. 9. The influence of Al^{3+} interlamellar concentration in partially exchanged Al-SAz-1 catalysts on Limonene conversion reaction conditions: 100 mg catalyst, 80 °C, 2 h, 1.5 ml MeOH, 0.5 ml Limonene.

3.7. The influence of the Al^{3+} interlamellar concentration

Additional experiments were performed in order to determine the influence of the extent of the ion-exchange process on limonene alkoxylation. We sought to clarify whether all the Al-ions are equally active in the process or whether there are some specific sites, more active than the others, e.g. those which Al-ions populate first. The catalysts were prepared using the Na-form of SAz-1 which was treated with sufficient Al^{3+} ions to satisfy 10, 20, 30, 50, 70 and 100% of the CEC. Fig. 9 illustrates the results in the form of a plot of limonene conversion against interlamellar Al^{3+} concentration, expressed as meq/100 of dry clay.

Surprisingly, there was no catalytic activity at low Al contents (up to 20% of CEC). When more than 30% of the CEC is occupied by Al-ions, the catalytic activity begins to increase. Since this reaction is proton catalyzed, the shape of the correlation after the threshold value reflects changes in the active proton concentration as a function of the interlamellar Al^{3+} concentration. These results are very similar to those reported by Purnell et al. [29] for the dehydration of pentan-1-ol to form the di-pentyl ether and 2-pentene over co-ionic Na^{+}-Al^{3+}-exchanged clays.

4. Conclusion

Modified clays have been proposed as active and selective catalysts for the synthesis of α-terpinyl methyl ether by alkoxylation of limonene with methanol. The GC-MS analysis of the reaction mixtures showed that α-terpinyl methyl ether was obtained with good selectivity over the proposed clay-based catalysts. Among the different reaction parameters, temperature plays an important role, with the best selectivity being recorded at temperatures below 50 °C. The reaction was performed over catalysts prepared from different starting clays, activated using ion-exchange and by acid treatment. By performing the reaction over different ion-exchanged and acid activated clays, the key characteristics of the catalysts have been identified. Thus, the co-existence of Brønsted acid sites and of a 2-D gallery, as in the Al^{3+}-exchanged and/or mildly acid activated clays, favor the alkoxylation reaction.

Acknowledgements

This research was supported by FCT with funds from the Portuguese Government (Projects PEst-OE/QUI/UI0674/201, Pest-OE/QUI/UI619/2011 and PTDC/CTM-CER/121295/2010 (CLAY-CATS4 – Clay catalysts for biomass conversion)).

Appendix A. Supplementary data

Supplementary data associated with this article can be found, in the online version, at http://dx.doi.org/10.1016/j.apcata.2013.07.012.

References

[1] A.F. Thomas, Y. Bessiere, Nat. Prod. Rep. 6 (1989) 291–309.
[2] K. Hensen, C. Mahaim, W.F. Hölderich, Appl. Catal. A: Gen. 149 (1997) 311–329.
[3] W.F. Hölderich, D. Heinz, in: J.J. Spivey (Ed.), Catalysis, The Royal Society of Chemistry Vol. 14 (1999) 148–182.
[4] M. Stanciulescu, M. Ikura, J. Anal. Appl. Pyrol. 75 (2006) 217–225.
[5] M. Stanciulescu, M. Ikura, J. Anal. Appl. Pyrol. 78 (2007) 76–84.
[6] J.M. Adams, R.W. McCabe, in: R.A. Schoonheydt, C.T. Johnston (Eds.), Handbook of Clay Science, Elsevier, 2006, pp. 541–581.
[7] F. Bergaya, B.K.G. Theng, G. Lagaly, in: R.A. Schoonheydt, C.T. Johnston (Eds.), Handbook of Clay Science, Elsevier, 2006, pp. 261–421.
[8] C. Breen, Clay Miner. 26 (1991) 473–486.
[9] M. Janek, P. Komadel, Geol. Carpath. 50 (1999) 373–378.
[10] P. Botella, A. Corma, J.M.L. Nieto, S. Valencia, M. Lucas, M. Sergio, Appl. Catal. A: Gen. 203 (2000) 251–258.
[11] S. Kaufhold, R. Dohrmann, M. Klinkenberg, S. Siegesmund, K. Ufer, J. Colloid Interface Sci. 349 (2010) 275–282.
[12] D.W. Rutherford, C.T. Chiou, D.D. Eberl, Clays Clay Miner. 45 (1997) 534–543.
[13] L.J. Michot, F. Villiéras, Surface area and porosity, in: R.A. Schoonheydt, C.T. Johnston (Eds.), Handbook of Clay Science, Elsevier, 2006, pp. 965–978, Chapter 12.
[14] C. Breen, A.T. Deane, J.J. Flynn, Clay Miner. 22 (1987) 169.
[15] J.A. Ballantine, P. Graham, I. Patel, J.H. Purnell, K.J. Williams, J.M. Thomas, in: L.G. Schultz, H. van Olphen, F.A. Mumpton (Eds.), Proceedings of the International Clay Conference, Denver, 1985, The Clay Minerals Society, Bloomington, IN, 1987, p. p.311.
[16] C. Catrinescu, C. Fernandes, P. Castilho, C. Breen, Appl. Catal. A: Gen. 311 (2006) 172–184.
[17] F. Annabi-Bergaya, M.I. Cruz, L. Gatineau, J.J. Fripiat, Clay Miner. 16 (1981) 115–122.
[18] E. Royals, J. Am. Chem. Soc. 71 (1949) 2568–2571.
[19] R.S. Karinen, J.A. Linnekoski, A.O.I. Krause, Catal. Lett. 76 (2001) 81–87.
[20] I. Bardyshev, L. Popova, Zh. Org. Khim. 30 (1994) 970–978.
[21] K. Hensen, C. Mahaim, W.F. Holderich, Appl. Catal. A: Gen. 149 (1997) 311–329.
[22] D.R. Brown, C.N. Rhodes, Catal. Lett. 45 (1997) 35–40.
[23] M.P. Hart, D.R. Brown, J. Mol. Catal. A: Chem. 212 (2004) 315–321.
[24] C. Breen, J. Madejova, P. Komadel, J. Mater. Chem. 5 (1995) 469–474.
[25] P. Komadel, M. Janek, J. Madejova, A. Weekes, C. Breen, J. Chem. Soc., Faraday Trans. 93 (1997) 4207–4210.
[26] C. Breen, J. Madejova, P. Komadel, Appl. Clay Sci. 10 (1995) 219–230.
[27] C. Breen, F.D. Zahoor, J. Madejova, P. Komadel, J. Phys. Chem. B 101 (1997) 5324–5331.
[28] C. Fernandes, C. Catrinescu, P. Castilho, P.A. Russo, M.R. Carrott, C. Breen, Appl. Catal. A: Gen. 318 (2007) 108–120.
[29] J.H. Purnell, J.M. Thomas, P. Diddams, J.A. Ballantine, W. Jones, Catal. Lett. 2 (1989) 125–128.
[30] S. Brunauer, P.H. Emmett, E. Teller, J. Am. Chem. Soc. 60 (1938) 309–319.
[31] F. Rouquerol, J. Rouquerol, K. Sing, Adsorption by Powders and Porous Solids, Academic Press, London, 1999.
[32] S.J. Gregg, K.S.W. Sing, Adsorption, Surface Area and Porosity, Academic Press, London, 1982.